Mechanism of Hollow Nanoparticle Formation Due to Shape Fluctuations

J. Erlebacher[1,*] and D. Margetis[2]
[1]Materials Science and Engineering, Johns Hopkins University, Baltimore, Maryland 21218, USA
[2] Mathematics, and Institute for Physical Science and Technology, and Center for Scientific Computation and Mathematical Modeling, University of Maryland, College Park, Maryland 20742, USA
(Received 31 May 2013; published 18 April 2014)

Shape fluctuations in nanoparticles strongly influence their stability. Here, we introduce a quantitative model of such shape fluctuations and apply this model to the important case of Pt-shell/transition metal-core nanoparticles. By using a Gibbs distribution for the initial shapes, we find that there is typically enough thermal energy at room temperature to excite random shape fluctuations in core-shell nanoparticles, whose amplitudes are sufficiently high that the cores of such particles are transiently exposed to the surrounding environment. If this environment is acidic and dissolves away the core, then a hollow shell containing a pinhole is formed; however, this pinhole quickly closes, leaving a hollow nanoparticle. These results favorably compare to experiment, much more so than competing models based on the room-temperature Kirkendall effect.

DOI: 10.1103/PhysRevLett.112.155505 PACS numbers: 61.46.Df, 82.47.-a

There are a number of recent observations of hollow nanoparticles formed via the Kirkendall effect in annealed core-shell nanoparticles, i.e., uncompensated high-temperature bulk interdiffusion between the core and the shell [1]. This effect is certainly operative when the final shell composition is an alloy mixture of the two components [2]. Recently, however, the Kirkendall effect has been implicated in the formation of hollow Pt-shell nanoparticles formed from Pt-shell/transition metal (e.g., Ni) core nanoparticles in electrolytes at room temperature [3–6]. This class of nanoparticles is useful in many low-temperature electrochemical reactions, such as oxygen reduction in fuel cells. This "room temperature Kirkendall effect" (rt-KE) is invoked in systems that differ from the high-temperature phenomena in an important way: the shell that is observed to remain after electrochemical processing, which serves to dissolve away any surface Ni, is comprised of pure Pt.

In this Letter, we argue that the kinetics of vacancy-mediated diffusion in core-shell nanoparticles at room temperature are far too slow to justify attribution of the formation of Pt-shell hollow nanoparticles in electrochemical environments to the rt-KE. We present an alternative model (Fig. 1) in which thermal energy induces surface-diffusion mediated random fluctuations in the shape of Pt-shell nanoparticles, fluctuations whose amplitudes are high enough to expose the core, forming pinholes in the shell and allowing the cores to be dissolved away. Once the cores are dissolved away, the mismatch of interior and exterior curvatures provides a new driving force for surface diffusion through the pinholes that closes them rapidly.

In early studies of dealloying (dissolving the less noble component out of a two-component alloy), it was hypothesized that the less noble component might be transported to the surface via a bulk vacancy diffusion mechanism [7]. However, the site concentration of vacancies $e^{-\Delta G_v/(k_B T)}$, where ΔG_v is the vacancy formation energy ($\Delta G_v = 1.15$ eV for Pt), is orders of magnitude too low at room temperature (1 vacancy per 3×10^{19} atoms;

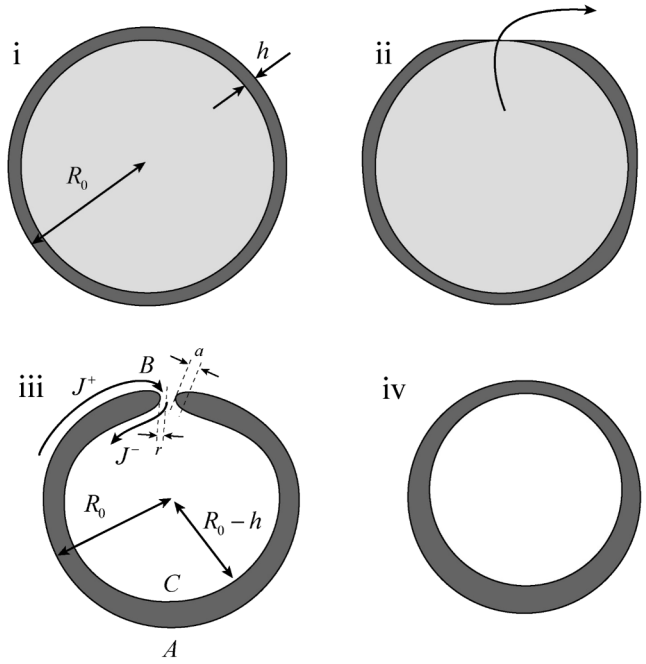

Fig. 1 Stages in the surface-diffusion driven formation of hollow nanoparticles. (i) A core-shell nanoparticle of radius R_0 and shell thickness h; (ii) shape fluctuations in the outer surface expose the core, allowing it to be dissolved away; (iii) a pinhole of radius r exists in the shell, but quickly closes up because of a diffusional flux from the convex outer surface A through the pinhole edge B and into the inner concave surface C. (iv) When the radius of curvature of the pinhole edge a becomes sufficiently large, the net flux at the pinhole edge $J^+ - J^-$ is positive, closing the pinhole and leaving a hollow nanoparticle.

equivalent to one vacancy in 8×10^{14} 10 nm-diameter Pt nanoparticles) [8]. Similarly, the bulk migration energy ($\sim$1.5 eV) yields bulk diffusion coefficients of order 10^{-27} cm^2/ sec [9]; this is geologically slow in comparison to the minutes time scale of the rt-KE. To account for higher vacancy concentrations in Pt-shell particles in acid electrolytes, it is hypothesized that experimental procedures lead to an excess of vacancies at the core-shell interface; similarly, fast vacancy diffusion can be induced in simulation, but only by imposing unrealistically high driving forces [10]. Dealloying has subsequently been shown to be controlled by surface diffusion [11], so it is reasonable to explore whether a similar mechanism can be invoked for core-shell nanoparticles at room temperature, without resorting to the rt-KE.

In contrast to kinetic growth problems [12], we hold the nanoparticle volume constant, with a steady-state spherical shape. We focus on small random fluctuations around this steady-state shape. Such small fluctuations have long been observed in experiment [13], and resemble vesicle deformations analyzed as a free-boundary problem [14]. We assume uniform surface energy γ, leading to a spherical Wulff shape. The assumption regarding kinetics is that the shape evolves only via surface diffusion, so that the normal velocity v_n of the surface is [15]

$$v_n = -M\Delta_S\kappa. \tag{1}$$

Here, $\kappa = (\kappa_1 + \kappa_2)/2$ is the mean curvature (the arithmetic mean of principal curvatures κ_1 and κ_2), Δ_S is the surface Laplacian, and $M = C_{\rm surf}D\Omega^2\gamma/(k_BT)$ is the mobility associated with surface diffusion, where $C_{\rm surf}$ is the areal concentration of diffusers, D is the surface diffusion coefficient, and Ω is the atomic volume. A stochastic noise term could be added to Eq. (1), rendering the analysis significantly complex. This approach does not provide fundamentally different insights than what we report here.

Our simplified approach relies on using Eq. (1) with random initial nanoparticle shapes. We consider an ensemble of initial axisymmetric shapes that form small perturbations of a sphere of radius R_0; these remain axisymmetric by evolution under Eq. (1). In the spirit of [14], let $\rho(s,t)$ be the distance of any point on the surface from the axis (say, z axis) of rotation, where s is the arc length of the contour that generates the surface and t is time; $0 \le s \le s_m(t)$ and $\rho(s_m(t),t) = 0$. We consider the deterministic evolution of a perturbed sphere from an initial time ($t = 0$) for which $\rho(s,0) = R_0\sin(s/R_0) + \varepsilon\psi_0(s)$, $0 < \varepsilon \ll 1$; as a result, we expect that at any later time, $t > 0$, $\rho(s,t) = R_0\sin(s/R_0) + \varepsilon\psi^{(1)}(s,t) + \varepsilon^2\psi^{(2)}(s,t) + \cdots$, where each $\psi^{(k)}$ ($k = 1, 2, \ldots$) has units of length. For our purposes, it suffices to compute only $\psi^{(1)}(s,t)$, which we determine via the mean curvature expansion $\kappa(s,t) = 1/R_0 + \varepsilon\kappa^{(1)}(s,t) + \cdots$. By Eq. (1), this $\kappa^{(1)}(s,t)$ satisfies [14] $\partial_t\kappa^{(1)} = -(M/2)[\Delta_0^2 + 2R_0^{-2}\Delta_0]\kappa^{(1)}$, where Δ_0 is the Laplacian on the sphere of radius R_0, $\Delta_0 = \partial_{ss} + R_0^{-1}\cot(s/R_0)\partial_s$, $0 \le s \le \pi R_0$, and ∂_s denotes the partial derivative $\partial/\partial s$. We apply an expansion of $\kappa^{(1)}$ in spherical harmonics $Y_{l0}(\theta)$ with mode amplitudes K_l viz.,

$$\kappa^{(1)}(s,t) = R_0^{-2}\sum_{l=2}^{\infty} K_l Y_{l0}(\theta)e^{-\alpha_l^2 Mt/(2R_0^4)}, \tag{2}$$

where $\alpha_l^2 = (l-1)l(l+1)(l+2)$, $l \ge 2$, and $0 \le \theta = s/R_0 \le \pi$ (θ: polar angle). By definition of the mean curvature, we obtain $\partial_{\theta\theta}\psi^{(1)} + \psi^{(1)} = -2R_0^2\kappa^{(1)}\sin\theta$, which yields the time-dependent shape of the perturbed particle [14]:

$$\psi^{(1)}(s,t) = \sum_{l=2}^{\infty} C_l\hat{\psi}_l(\theta)e^{-\alpha_l^2 Mt/(2R_0^4)}, \quad C_l = -2K_l; \tag{3}$$

C_l has units of length and the (non-dimensional) $\hat{\psi}_l(\theta)$ is the lth-mode shape function,

$$\hat{\psi}_l(\theta) = -\cos\theta\int_0^{\theta} Y_{l0}(\theta')\sin^2\theta'\,d\theta' + \sin\theta\int_0^{\theta} Y_{l0}(\theta')\sin\theta'\cos\theta'\,d\theta'. \tag{4}$$

Equations (3) and (4) describe the leading-order correction for the shape function given the amplitudes C_l, which can be extracted from $\psi_0(s)$ or $\kappa^{(1)}(s,0)$. Random fluctuations are induced by imposing random C_l in the initial condition via the Gibbs distribution at $t = 0$. By writing the total energy of the perturbed particle as $E(t) = 4\pi R_0^2\gamma + \mathsf{E}(t)$, where $\mathsf{E}(0)$ depends on $\psi_0(s)$, we assume that the probability distribution of initial shapes $\psi_0(s)$, or mode amplitudes $\{C_l\}_{l=2}^{\infty}$, is $P[\psi_0] = Ze^{-\mathsf{E}(0)/(k_BT)}$ (Z: normalization constant). The statistics of shape fluctuations stem from Eq. (3). To express P in terms of $\{C_l\}_{l=2}^{\infty}$, consider the formula [15] $\dot{E} \equiv dE(t)/dt = -2\gamma\iint_S v_n\kappa dS$, where S is the nanoparticle surface. By Eqs. 1) and 2, we compute $\dot{E}(t) \approx -2\varepsilon^2 M\gamma\iint_S|\nabla_S\kappa^{(1)}|^2 dS = -\varepsilon^2(M\gamma/R_0^4)\times\sum_l[l(l+1)/(2l+1)]C_l^2e^{-\alpha_l^2Mt/R_0^4}$, which is integrated to yield

$$\mathsf{E}(t) \approx \gamma\sum_{l=2}^{\infty}[(2l+1)(l-1)(l+2)]^{-1}C_l^2e^{-\alpha_l^2Mt/R_0^4}. \tag{5}$$

Thus, $E(t)$ is a random variable for every t. In the steady-state limit, $E(t\to\infty) = 4\pi R_0^2\gamma$, we recover the surface energy of the unperturbed shape (the sphere). To derive Eq. (5), we have set $\varepsilon = 1$, which only requires that the standard deviation of C_l be small compared to R_0/l.

By the Gibbs distribution $P = Ze^{-\mathsf{E}(0)/(k_BT)}$; with Eq. (5), $P = \prod_l P_l$, where $P_l \propto e^{-\gamma[(2l+1)(l-1)(l+2)]^{-1}C_l^2/(k_BT)}$. Thus,

the random fluctuation amplitudes C_l are independent, each with zero mean ($\langle C_l \rangle = 0$) and variance $\langle C_l^2 \rangle = (1/2)(2l+1)(l-1)(l+2)k_BT/\gamma$. In order for the linear theory to hold, a reasonable criterion is that $(1/2)\sqrt{\langle C_l^2 \rangle} < R_0/l$, where R_0/l is of order the wavelength, so this linear model is valid for modes l such that

$$l < N \equiv (4\gamma R_0^2/k_BT)^{1/5}. \quad (6)$$

Equation (5) indicates that, for fixed perturbation amplitude C_l, the probability P_l of finding the lth fluctuation mode increases with l. This is expected physically, as high-l modes are associated with high spatial frequency fluctuations that require short-distance mass transport. Correspondingly, however, high-l fluctuations are also very short lived. Thus, the consideration of any nonlinearity is not expected to play a physically significant role in the mechanism of hollow particle formation discussed in this Letter.

In electrochemical experiments involving Pt-shell nanoparticles, the exterior surface of the particles is often cycled between potentials that form a surface oxide, leaving a surface comprised of PtO, and reducing potentials that leave a pure Pt surface. Values for the surface energies and atomic volumes of Pt, PtO, are $\gamma_{\mathrm{Pt}} = 15\ \mathrm{eV/nm^2}$, $\gamma_{\mathrm{PtO/Pt}} = 3.1\ \mathrm{eV/nm^2}$, $\Omega_{\mathrm{Pt}} = 1.5 \times 10^{-2}\ \mathrm{nm^3}$, $\Omega_{\mathrm{PtO}} = 2.5 \times 10^{-2}\ \mathrm{nm^3}$ [16,17]. We will focus our discussion on particles with radius $R_0 = 6.5$ nm and shell thickness of 2 nm, at $T = 298$ K, comparing to the data of Wang et al. [3]. For these parameters, Eq. (6) yields an upper bound for l near $N \sim 10$. Independent experimental measurements of C_{surf} and D have not been made. However, Martinez Jubrias *et al.* [17] experimentally measured the morphological relaxation times for roughened Pt surfaces as a function of temperature and electrochemical potential, yielding a range for the product DC_{surf} from 0.023 to 0.44 $\mathrm{sec^{-1}}$ over relevant electrochemical potentials from ~0.1 V (Pt) to ~1.1 (PtO) vs RHE (RHE: reversible hydrogen electrode). Note that significant details about activation barriers, formation energies, and particular diffusion pathways on Pt surfaces in contact with aqueous acidic electrolytes with adsorbed oxide species and solution anions are as-yet unknown for these systems, making modeling by kinetic Monte Carlo methods, for instance, difficult. Figure 2 shows the probability $F_l = 2\int_{C_*}^{\infty} P_l(C)dC$ that a fluctuation of mode l exceeds a critical amplitude C_*, for $C_* = 0.25$, 2.0 nm, for Pt- and PtO-terminated surfaces. Assuming the Gibbs distribution $P \propto e^{-\mathsf{E}(0)/(k_BT)}$ for the initial shapes, cf. Eq. (5), $F_l(C_*) = \mathrm{erfc}(\beta_l C_*)$, where $\beta_l = \sqrt{\gamma[(2l+1)(l-1)(l+2)]^{-1}/k_BT}$ and erfc is the complementary error function. For an amplitude of $C_* = 0.25$ nm (i.e., a 0.5 nm thick shell), P_l rises to nearly unity by $l \sim 10$ for both Pt and PtO surfaces. Even for an amplitude of $C_l = 2.0$ nm (a 4.0 nm thick shell), the probability P_l is greater than 50% at $l \sim 10$ for PtO surfaces, although this probability is lower for Pt surfaces.

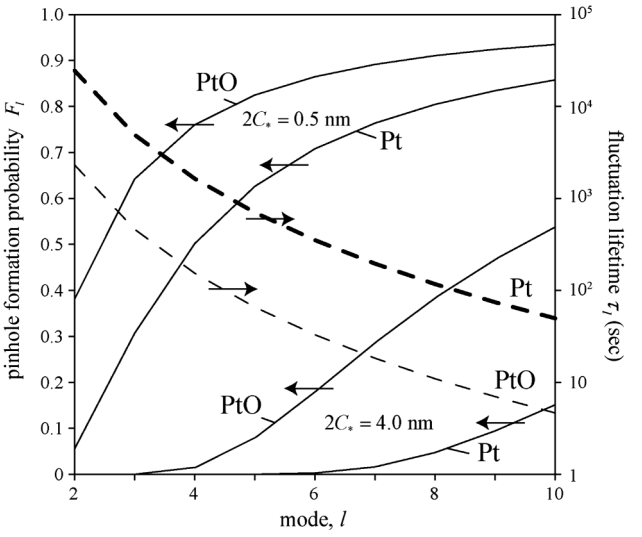

Fig. 2 (solid lines; left vertical axis): Pinhole formation probability F_l associated with generating a fluctuation with peak-to-valley length greater than threshold $2C_*$, vs fluctuation mode l. (dashed lines; right vertical axis): Fluctuation lifetime τ_l vs fluctuation mode l. Results are shown for Pt- and PtO-terminated surfaces, with shells of 0.5 and 4.0 nm thickness and core radius $R_0 = 6.5$ nm; in all cases, fluctuations are highly probable and possess lifetimes long enough to allow attack of the core by an external electrolyte.

At high potentials, dissolution of the core of 10 nm diameter particles is typically faster than 1 sec. For such dissolution to occur, the fluctuation lifetime must be longer. By the exponential in Eq. (5), the lifetime of the lth mode is estimated as $\tau_l = R_0^4 M^{-1} \alpha_l^{-2}$ and is plotted in Fig. 2 for Pt- and PtO-terminated surfaces. For nearly all modes, the lifetime of fluctuations is greater than 1 sec. (still, with a high probability of existence), rising to greater than 10^4 seconds for the very lowest mode ($l = 2$) on Pt-terminated surfaces. For shell thickness from 0.5 to 4.0 nm, we conclude that under reasonable conditions fluctuations are both sufficiently probable and long enough lived to expose the core to the surrounding electrolyte, allowing the cores to be dissolved away. This conclusion holds for both Pt-terminated and PtO-terminated surfaces. The PtO surface, however, is significantly more mobile than Pt. This fact may explain why the hollow Pt shell nanoparticles in Co_3Pt nanoparticles are seen only when the particles are subjected to high potential [4,6]. We also expect our conclusions to be qualitatively unaffected by including azimuthal modes.

To this point we have argued that pinholes in the nanoparticle Pt shells are inevitable. However, they are not observed experimentally [3], and their treatment must be considered separately from the shape fluctuations that

led to exposure of the core to the electrolyte. A simple kinetic model shows that small pinholes should close quite quickly. The central physical observation is that without the pinhole, curvature variations on the surface are relatively small, but once the core has been dissolved away, there is a significant new driving force for mass transport from the convex outer surface to the concave inner one; this driving force distinguishes this problem from that of pinhole closure in planar films [18]. Mass transport occurs via surface diffusion as follows: In good approximation, the geometry of a shell with a pinhole is characterized by the mean curvature at three points (labeled A, B, and C in Fig. 1). According to the Gibbs-Thomson relation, the chemical potential at each point is given by $\mu = \mu_\infty + \gamma\kappa\Omega$, where κ is the mean curvature as above, and μ_∞ is the reference chemical potential of a planar surface. Upon the formation of the pinhole, $\kappa_A = 1/R_0$ and $\kappa_C = -1/(R_0 - h)$, leading to an overall gradient in chemical potential that provides a driving force for mass transport from the outer surface to the inner one. At the pinhole edge $\kappa_B = (1/2)(1/a - 1/r)$, where r is the radius of the pinhole and $1/a$ is the curvature of the edge of the pinhole (Fig. 1). In principle, when the pinhole first opens, a may be very small, so that $\mu_B \gg \mu_A, \mu_C$, and the pinhole will open. However, this process blunts the edge of the pinhole, quickly increasing the magnitude of a to a value of order of the shell thickness h. For small pinholes, the $1/r$ term then will dominate the chemical potential of the pinhole. Note that the condition $r \ll h$ for closure of the pinhole does not violate our assumption of linearity which requires that the standard deviation of h be much smaller than R_0.

A simple analysis for the closure time of the pinhole follows: Quantitatively, if h is the shell thickness then the flux J^+ to the pinhole edge is

$$J^+ = -\frac{DC}{k_B T}\left[\frac{\mu_B - \mu_A}{\Delta x_1}\right] = -\frac{DC_{\text{surf}}\gamma\Omega^{2/3}}{k_B T}\left[\frac{1}{2}\left(\frac{1}{a} - \frac{1}{r}\right) - \frac{1}{R_0}\right]\frac{1}{(\pi R_0 - r)}. \quad (7)$$

This is a minimum flux, because we assume the distance Δx_1 over which the gradient is measured is maximal, equal to the distance from the pinhole edge to the point A on the particle farthest away from the edge, i.e., $\Delta x_1 = \pi R_0 - r$, and we have related the volumetric concentration of diffusers C to the surface concentration C_{surf} using $C_{\text{surf}} = C\Omega^{1/3}$. An expression similar to Eq. (7) can be written for the flux J^- between the pinhole edge and the inner surface using $\Delta x_2 = \pi(R_0 - h) - r$. For large enough a/r_0, one finds that the net flux $J_{\text{net}} = J^+ - J^-$ to the pinhole edge is always positive, consistent with the notion that pinholes should shrink. In the limit of small r/R_0 and h/R_0, this net flux is given by $J_{\text{net}} = [DC_{\text{surf}}\gamma\Omega^{2/3}/(\pi R_0 k_B T)](1/r - 1/a)$. Mass conservation relates the shrinkage rate dr/dt of the pores to the net flux as $dr/dt = -J_{net}\Omega$, allowing us to determine the closure time t_c, i.e., the time elapsed during a change in pinhole radius from $r = r_0$ to $r = 0$:

$$t_c = \left(\frac{\pi a R_0 k_B T}{DC_{\text{surf}}\gamma\Omega^{5/3}}\right)\left(a \ln\left|\frac{a}{a - r_0}\right| - r_0\right). \quad (8)$$

Again, as we have taken the longest diffusion path possible, Eq. (8) is an approximate upper bound for the closure time. Figure 3 shows the closure time t_c vs initial pinhole radius r_0 for $R_0 = 6.5$ nm in shells comprised of Pt and PtO surfaces, for various values of the pinhole edge curvature a^{-1} ($r_0 < a$). Pinholes in PtO-terminated surfaces close very quickly; except when the pinholes have radius greater than 1 nm, they will close up within order of 100 sec., i.e., shorter than the time of typical experiments such as described in Ref. [3]. Pt-terminated surfaces close more slowly, consistent with their smaller mobility, but even here we can expect pinholes of radius 0.5 nm to close up within order of 100 sec.

In this Letter, we have argued in favor to an alternative to the room-temperature Kirkendall effect in core-shell nanoparticles. Especially for the technologically relevant case of Pt nanoparticles, we showed that surface fluctuations are highly probable and lead to exposure of nanoparticle cores. When these cores dissolve, any pinholes in the shell quickly close. The model here is minimal, partly based on the reasonable assumptions of an initial Gibbs distribution and small shape fluctuations, and may be further

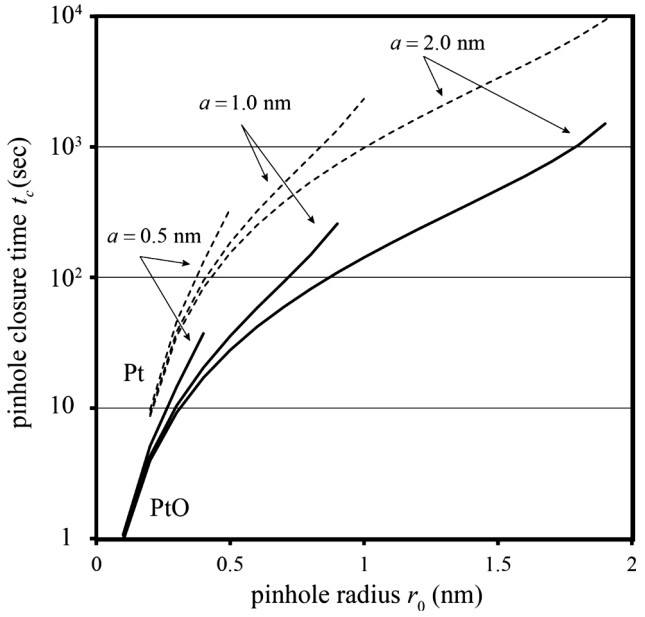

Fig. 3 Pinhole closure time t_c vs initial pinhole radius r_0 for different values of the pinhole edge radius of curvature a. PtO-terminated surfaces: thick lines; Pt-terminated surfaces: thin dashed lines.

refined by including effects of anisotropic surface energy and/or effects associated with steps, terraces, and facet boundaries on particle surfaces. More broadly, this work confirms the dynamic nature of nanoparticle shapes seen in microscopy and electrochemical measurements, and quantifies the degree to which thermal fluctuations can impact the stability and lifetime of structurally complex nanoparticles.

The authors are grateful to the NSF for financial support under programs DMR-1003901 (J. E.) and DMS-0847587 (D. M.).

*Corresponding author.

[1] H. J. Fan, U. Gosele, and M. Zacharias, Small **3**, 1660 (2007).
[2] A. M. Gusak and K. N. Tu, Acta Mater. **57**, 3367 (2009).
[3] J. X. Wang, C. Ma, Y. M. Choi, D. Su, Y. Zhu, P. Piu, R. Si, M. B. Vukmirovic, Y. Zhang, and R. R. Adzic, J. Am. Chem. Soc. **133**, 13 551 (2011).
[4] L. Dubau, J. Durst, F. Maillard, L. Guetaz, M. Chatenet, J. Andre, and E. Rossinot, Electrochim. Acta **56**, 10 658 (2011).
[5] X. Zhou, Y. Gan, J. Du, D. Tian, R. Zhang, C. Yang, and Z. Dai, J. Power Sources **232**, 310 (2013).
[6] M. Lopez-Haro, L. Dubau, L. Guetaz, P. Bayle-Guillemaud, M. Chatenet, J. Andre, N. Caque, E. Rossinot, F. Maillard, Appl. Catal., B **152–153**, 300 (2014).
[7] H. W. Pickering and C. Wagner, J. Electrochem. Soc. **114**, 698 (1967).
[8] R. M. Emrick, J. Phys. F **12**, 1327 (1982).
[9] D. Schumacher, A. Seeger, and O. Harlin, Phys. Status Solidi **25**, 359 (1968).
[10] R. Callejas-Tovar, C. Alex Diaz, J. M. Martinez de la Hoz, and P. B. Balbuena, Electrochim. Acta **101**, 326 (2013).
[11] J. Erlebacher, M. J. Aziz, A. Karma, N. Dimitrov, and K. Sieradzki, Nature (London) **410**, 450 (2001).
[12] W. W. Mullins and R. F. Sekerka, J. Appl. Phys. **34**, 323 (1963).
[13] L. D. Marks, Rep. Prog. Phys. **57**, 603 (1994).
[14] R. Rosso, Interface Free Bound. **3**, 345 (2001).
[15] J. Cahn and J. E. Taylor, Acta Metall. Mater. **42**, 1045 (1994).
[16] L. Tang, X. Li, R. C. Cammarata, C. Friesen, and K. Sieradzki, J. Am. Chem. Soc. **132**, 11 722 (2010).
[17] J. J. Martinez Jubrias, M. Hidalgo, M. L. Marcos, J. Gonzalez Velasco, Surf. Sci. **366**, 239 (1996).
[18] M. Lanxner and C. L. Bauer, Thin Solid Films **150**, 323 (1987).